X-ray and Ultrasound Data Fusion

Stéphane Gautier
EDF-DER, 6 quai Watier, F 78401 Chatou Cedex.
Stephane.Gautier@der.edfgdf.fr

Jérôme Idier
LSS, ESE, Plateau de Moulon, F 91192 Gif sur Yvette Cedex
Jerome.Idier@lss.supelec.fr

Ali Resa Djafari
LSS, ESE, Plateau de Moulon, F 91192 Gif sur Yvette Cedex
Ali.Djafari@lss.supelec.fr

Blandine Lavayssière
EDF-DER, 6 quai Watier, F 78401 Chatou Cedex.
Blandine.Lavayssiere@der.edfgdf.fr

Abstract

This work deals with three dimensional reconstruction from X-ray and ultrasonic images. Such an issue pertains to the field of data fusion since the data provide complementary information. The two sets of data are independently related to two sets of parameters: X-ray attenuation and ultrasonic reflectivity. The fusion problem is adressed in a Bayesian framework; the kingpin of the task is to define a joint prior model for both attenuation and reflectivity. Dealing with the joint prior model, we propose to correlate the derivative of the attenuation and the reflectivity. Processing examples demonstrate the validity of the fusion approach and the robustness of the proposed method mismatching of the two sets of data.

1. Introduction

This paper deals with a data fusion method applied to the 3D reconstruction of an object from X-ray and ultrasonic data. The application of this work is the inspection of a steel block. In order to account for real conditions of inspection, only the upper face is accessible. The experimentation conditions for radiography are such that the X-ray scanning angle is reduced to 20°; thus the X-ray images provide mostly information along the lateral direction and they bring little information along the vertical direction. In order to reduce this lack of information, ultrasonic data are collected on the top of the block with a 0° incidence; since they are sensitive to horizontal breaks in the medium, they provide information along the vertical direction. In such a case, X-ray and ultrasound produce complementary information (see figure 1).

This fusion problem is similar to ones encountered in the field of biomedical imaging. It is for example the case when Positon Emssion Tomography (PET) and Magnetic Resonance Imaging (MRI) data are to be fused. With a fusion point of view, PET and MRI can respectively be compared to X-ray and ultrasonic imaging. For such applications, a sequential fusion process is mostly chosen [4]. MRI data are first processed, so as to obtain information about the breaks in the desired structure. Then, an activity map (that is similar to attenuation) is reconstructed from the PET data.

We believe it is essential to process jointly the two sets of data, so as to take the best advantage from the complementarity of the data. Firstly, we explain how specific the fusion problem is. Then, we expose the proposed method. The two sets of data are related with two independent sets of parameters: the attenuation for X-ray and the reflectivity for ultrasonic imaging. We propose to estimate jointly attenuation and reflectivity. Finally, processing results for real data sets are presented.

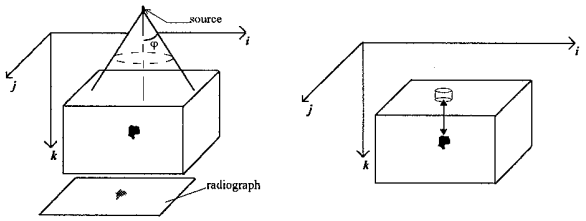

Fig. 1. Inspection conditions for X-ray and ultrasonic imaging.

2. Specificity of fusion

The problem is addressed in a Bayesian framework. Formally, the fusion can be considered as the estimation of an object $\boldsymbol{o}$, indirectly observed through two measurement systems that deliver the data $\boldsymbol{d}_1$ and $\boldsymbol{d}_2$. Calculating the data from a known object is called the *direct problem*. For the two data sets, we define the observation models M_1 and M_2 that respectively describe the related direct problems.

The estimation of the unknown object leads us to solve an *inverse problem*: the object is to be obtained from the measurements. Here, the existence, the uniqueness and the stability of the solution are not guaranteed: the inverse problem is *ill posed*. Then, in order to obtain an "acceptable" solution, some prior information about the searched object must be accounted for: the problem must be regularised [3]. In the Bayesian framework, this

0-8186-8821-1/98 $10.00 © 1998 IEEE

information is introduced through the object prior probability law $p(\boldsymbol{o})$. So, the whole available information about the object is contained in the joint law $p(\boldsymbol{o},\boldsymbol{d}_1,\boldsymbol{d}_2;\mathrm{M}_1,\mathrm{M}_2)$, obtained thanks to the Bayes' rule:

$$p(\boldsymbol{o},\boldsymbol{d}_1,\boldsymbol{d}_2;\mathrm{M}_1,\mathrm{M}_2) = p(\boldsymbol{d}_1,\boldsymbol{d}_2|\boldsymbol{o};\mathrm{M}_1,\mathrm{M}_2)p(\boldsymbol{o}).$$

This law depends both on the data, through the likelihood $p(\boldsymbol{d}_1,\boldsymbol{d}_2|\boldsymbol{o};\mathrm{M}_1,\mathrm{M}_2)$, and on the prior information given through the prior density $p(\boldsymbol{o})$. Since the two sets of data are obtained separately, the data likelihood can be split and the joint law is given by:

$$p(\boldsymbol{o},\boldsymbol{d}_1,\boldsymbol{d}_2;\mathrm{M}_1,\mathrm{M}_2) = p(\boldsymbol{d}_1|\boldsymbol{o};\mathrm{M}_1)p(\boldsymbol{d}_2|\boldsymbol{o};\mathrm{M}_2)p(\boldsymbol{o}).$$

Concretely, we aim above all at obtaining a solution to the inverse problem: a pointwise estimator is defined from the posterior distribution $p(\boldsymbol{o}|\boldsymbol{d}_1,\boldsymbol{d}_2;\mathrm{M}_1,\mathrm{M}_2)$. In the following, we decide on the maximum *a posteriori* estimator (MAP estimator) which maximises the posterior distribution.

Thus, the Bayesian approach enables, at least formally, to fuse different information sources corresponding to several data sets. Just like for any imaging inverse problem, the direct and the prior models are still to be defined with a wish to obtain the solution though a realistic algorithm.

From the foregoing, one could think the use of the Bayes' rule suppresses any specificity to the fusion problem; just like for any classical inversion problem, the use the Bayes' rule would erase any additional difficulty introduced through the fusion. In fact, a specific difficulty still remains for the fusion.

Indeed, here, the above so called "object" in fact indicates two "sub-object" $\boldsymbol{o}_1$ and $\boldsymbol{o}_2$, which are the attenuation map and the ultrasonic reflectivity. This definition is required to account for the direct models M_1 and M_2. The two parameter subsets characterise the same object but represent two different physical quantities. With such a viewpoint, our study is different from other fusion problems where indeed, different information sources are taken in account, but where the estimated parameters are physically homogeneous. In our case, each direct model relates one parameter set $\boldsymbol{o}_i$ with a data set $\boldsymbol{d}_i$. The joint law is the following:

$$p(\boldsymbol{o},\boldsymbol{d}_1,\boldsymbol{d}_2;\mathrm{M}_1,\mathrm{M}_2) = p(\boldsymbol{d}_1|\boldsymbol{o}_1;\mathrm{M}_1)p(\boldsymbol{d}_2|\boldsymbol{o}_2;\mathrm{M}_2)p(\boldsymbol{o}_1,\boldsymbol{o}_2).$$

Thus, the prior model definition requires the search for a link between the attenuation and the reflectivity. Indeed, this model cannot be reduced to two independent prior models for the sub-object: in such a case, $\boldsymbol{o}_1$ and $\boldsymbol{o}_2$ would be estimated separately and the fusion problem would disappear. The kingpin of the fusion is to define a joint prior model $p(\boldsymbol{o}_1,\boldsymbol{o}_2)$ linking the two sub-objects.

Since no physical models relates $\boldsymbol{o}_1$ and $\boldsymbol{o}_2$, the definition of a link between the attenuation and the reflectivity is one of the main difficulty of our work.

3. Joint fusion method

The definition of joint prior model for the attenuation and the reflectivity enables the joint estimation of these quantities. The joint solution is obtained through the minimisation of a compound criterium which depends both on the likelihood of the two data sets and on an additional part accounting for the attenuation and the reflectivity joint prior model. Firstly, the chosen direct models for the two imaging systems are defined. Then, we discuss the definition of the joint prior model. Finally, we give some details about the proposed minimisation algorithm.

The attenuation $\boldsymbol{x}$ and the reflectivity $\boldsymbol{r}$ are respectively related to the X-ray data $\boldsymbol{y}$ and the ultrasonic data $\boldsymbol{z}$. Each set of data is related to the object through the direct models $\boldsymbol{y} = \boldsymbol{A}\boldsymbol{x} + \boldsymbol{b}$ et $\boldsymbol{z} = \boldsymbol{H}\boldsymbol{r} + \boldsymbol{n}$; the operators $\boldsymbol{A}$ and $\boldsymbol{H}$ are respectivaly a projection and a convolution matrix; the noise processes $\boldsymbol{b}$ and $\boldsymbol{n}$ stand for the observation and direct model errors; they are supposed to be white, Gaussian and independent from $\boldsymbol{x}$ et $\boldsymbol{r}$; moreover, since the data are obtained separately, we suppose $\boldsymbol{b}$ and $\boldsymbol{n}$ are independent.

In such conditions, the joint MAP solution reads:

$$(\hat{\boldsymbol{x}},\hat{\boldsymbol{r}}) = \arg\min_{(\boldsymbol{x},\boldsymbol{r})}\left\{\|\boldsymbol{y}-\boldsymbol{A}\boldsymbol{x}\|^2 + \beta\|\boldsymbol{z}-\boldsymbol{H}\boldsymbol{r}\|^2 + U_{\mathrm{FU}}(\boldsymbol{x},\boldsymbol{r})\right\},$$

where β is a parameter whose value depends on the relative confidence in each data set; $U_{\mathrm{FU}}(\boldsymbol{x},\boldsymbol{r})$ stands for the prior model and thus enables a prior link between $\boldsymbol{x}$ and $\boldsymbol{r}$.

The search for the prior model is based on simple qualitative information. It can be considered that the object attenuation consists of homogeneous zones (steel and possible defects) and mostly of steel. Moreover, since the reflectivity accounts for discontinuities along the vertical direction and the object is made of homogeneous zones, it can be presumed that most reflectivities are zero-valued. Dealing with the link between the attenuation and the reflectivity, we can suppose a big reflectivity is connected with a break in the attenuation along the vertical direction; moreover, the reflectivities within the same zone of the attenuation should be very small. Such information about the links between $\boldsymbol{x}$ and $\boldsymbol{r}$ suggests introducing a correlation between the reflectivity and the vertical derivation of the attenuation.

Thus, the general scheme for the joint prior potential is given by:

$$U_{\mathrm{FU}}(\boldsymbol{x},\boldsymbol{r}) \propto \lambda_{\mathrm{GA}}\sum_{(s,t)\in H}\rho_{\mathrm{GA}}(x_s - x_t) + \lambda_{\mathrm{RAP}}\sum_{s\in S}\rho_{\mathrm{RAP}}(x_s - 1)$$
$$+\lambda_{\mathrm{FU}}\sum_{i,j,k}\rho_{\mathrm{FU}}(x_{i,j,k+1} - x_{i,j,k}, r_{i,j,k}),$$

where S denotes the set of sites s and H is the set of

horizontal neighbour sites. The functions ρ_{GA} and ρ_{RAP} account respectively for the attenuation homogeneity along the lateral directions and for the domination of steel in the object: they can be chosen among classical regularisation functions [2] [7]. The bivariate function $\rho_{FU}(u,r)$ enables to model both the spikiness of the reflectivity and the link between the attenuation and the reflectivity: it is the core of the joint potential definition.

Since the main contribution of this paper deals with the linking between the attenuation and the reflectivity, we insist especially on the choice of the $\rho_{FU}(u,r)$ function.

So as to link the derivative of the attenuation, it can first be thought of defining ρ_{FU} as $\rho_{FU}(u,r) = \rho(|u| - \alpha|r|)$, where ρ is a scalar regularisation function. Still, such functions create scale problems between $\boldsymbol{x}$ et $\boldsymbol{r}$ and the choice for α may happen to be difficult. We therefore focus on functions that introduce a more flexible link between the attenuation and the reflectivity.

We can for example extend the truncated quadratic function [1] to the bivariate case, choosing:

$$\rho_{FU1}(u,r) = \min(u^2 + \alpha^2 r^2, T).$$

This function is quadratic as long as the sum $u^2 + \alpha^2 r^2$ is smaller that T and is constant out of this zone (see fig. 2). The parameter α makes it possible to adapt the model to different scales between $\boldsymbol{x}$ and $\boldsymbol{r}$; T stands for the threshold above which a jump in the attenuation and the reflectivity is allowed. This model owns some of the seeked properties. Indeed, when the variables are to small, the smoothing effect of the quadratic function is efficient and, in the same time, high values for the variables are not penalised too much. Still, the correlations introduced in this model are probably too strong to obtain a method which should be robust towards geometrical matching troubles between the two sets of data.

Indeed, it is shown in [6] that the prior model's complexity should be adapted to the richness of the data; thus, accounting both for the poor information in our data and our will to obtain a method that is robust with respect to choice of the hyperparameters λ, we want to obtain a convex potential function and so we choose convex functions ρ. We are especially searching for a function that introduces looser links than the function ρ_{FU1}.

Taking advantage of the scalar hyperbolic function, we define the bivariate hyperbolic function as:

$$\rho_{FU2}(u,r) = \sqrt{T^2 + u^2 + (\alpha r)^2}.$$

This function is quadratic-like when both u and r are small enough and conical-like for big values of any of the two variables (see fig. 2). Thus, rare events such as a break in the attenuation or the occurrence of a high reflectivity are softly penalised. The parameter T makes it possible to enlarge or reduce the quadratic area; thus tuning T enables the choice for the strength of the link between $\boldsymbol{x}$ and $\boldsymbol{r}$. Tuning α adapts the model to different scales for u and r. Lastly, this bivariate function is jointly convex with respect to (u, r).

Finally, the U_{FU} potential is defined by:

$$U_{FU}(\boldsymbol{x},\boldsymbol{r}) = \lambda_{GA} \sum_{(s,t)\in H} \sqrt{T_{GA}^2 + (x_s - x_t)^2} + \lambda_{RAP} \sum_{s\in S} |x_s - 1|^{p_{RAP}} + \lambda_{FU} \sum_{i,j,k} \sqrt{T_{FU}^2 + \left(x_{i,j,k+1} - x_{i,j,k}\right)^2 + \alpha^2 r_{i,j,k}^2},$$

where β, λ_{GA}, T_{GA}, λ_{RAP}, p_{RAP}, λ_{FU}, T_{FU} and α are hyperparameters. The hyperparameter values are chosen empirically. The cost function to be minimised is globally convex with respect to $\boldsymbol{x}$ and $\boldsymbol{r}$; thus the solution is computed through a combined conjugate gradient algorithm.

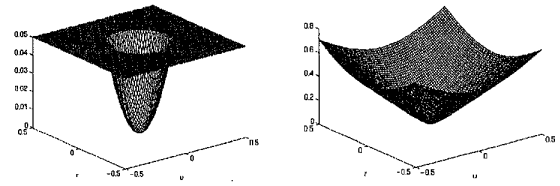

Fig. 2. Examples for the bivariate quadratic (left) and the bivariate hyperbolic (right) functions.

4. Processing results

The application deals with the inspection of an austeno-ferritic block. An electro-eroded known defect has been created in the block. The X-ray data have been obtained according to the conditions given in the introduction; the three sources' positions are so that the object is observed sideways (see fig.3).

So as to concentrate on the sole results of the fusion method, we need to get rid of the likely position mismatching between the two sets of data; moreover we also have to get rid of the difficult wavelet estimation step [6]. The processed ultrasonic traces are therefore simulated data obtained through the convolution model. Since the ultrasonic waves do not propagate in the air, the original reflectiviy has only one spike which accounts for the upper bound of the defect (see fig. 5a). The convolution kernel used for simulation is low pass (Ricker's wavelet) and the signal to noise ration is 0 dB. A typical ultrasonic trace is given in figure 5b.

The presented results for the attenuation are vertical slices of the reconstructed volumes. Since the block is observed sideways, the reconstructed defect is naturally slightly inclined. Moreover, since the X-rays belong to a narrow beam, the defect reconstructed from the sole radiographs is streched along the vertical direction (see fig. 4b).

Firstly, we study the global fusion method for the perfect positioning case. The results clearly prove how successful the fusion approach is (see fig. 4b and 4c). The estimated reflectivity is indeed correlated with the attenuation and it even contains some information about the bottom of the defect (see fig. 5c), whereas it was not introduced into the simulated traces; this second spike matches the low jump in the reconstructed attenuation. Those results also prove the method is robust towards mispositioning of the two sets of data ; indeed, even when the positioning is totally wrong, the artefact due to the positioning error is not important (see figure 4d), so that the reconstruction quality is nearly as good as when the sole radiographs are used (see figures 4b and 4d). Moreover, the proposed method is more robust towards positioning trouble than a sequential fusion method (see fig. 4b and 4e); in the later case, the two sets of data are processed separately [5] and the potential improvement provided by the fusion approach is drastically damaged.

At last, the empirical choice of hyperparameters is not a critical problem: the results are stable with respect to hyperparameter values. The hyperparameters chosen for the presented results are the following: $\lambda_{GA} = 10$, $T_{GA} = 0.005$, $\lambda_{RAP} = 2.5$, $p_{RAP} = 1.1$, $\lambda_{FU} = 10$, $T_{FU} = 0.005$, $\alpha = 1$, $\beta = 60$.

5. Conclusion

The fusion method we have proposed processes jointly the two data sets. The processing results prove how successful our approach is. For a perfect position matching, the fusion's contribution is undeniable. Moreover, the proposed method is robust towards positioning trouble, especially if compared with a sequential fusion method. Since we want to obtain a 3D representation of the object, we are only interested in the attenuation reconstruction, so the recovered reflectivity turns out to be a by-product of the method.

This method could be extended to other application fields such as biomedical imaging [8]. It should also be noticed the introduction of interactions between heterogeneous physical parameters, that are not related through a physical models, forms a generic set of problems.

6. References

[1] A. Blake, A. Zisserman. *Visual Reconstruction.* Cambridge, MA, MIT Press, 1987.

[2] C. Bouman, K. Sauer. A generalized gaussian image model for edge-preserving MAP estimation. *IEEE Trans. Image Processing*, vol.2:296-310, 1993.

[3] G. Demoment. Image reconstruction and restoration: overview of common estimation structures and problems. *IEEE Trans. Acoust., Speech, Signal Processing*, vol. 38:2024-2036, 1989.

[4] J. A. Fessler, N. H. Clinthorne, W. L. Rogers. Regularized emission image reconstruction using imperfect side information. *IEEE Trans. Nuclear Science*, vol. 39 : 1464-1471, 1992.

[5] S. Gautier, G. Le Besnerais, A. Mohammad-Djafari, B. Lavayssière. Data fusion in the field of non destructive testing. *Proc. of the 15th Int. MaxEnt Workshop,* SantaFe, NM, 1995.

[6] S. Gautier. *Fusion de données gammagraphiques et ultrasonores. Application au contrôle non destructif.* PhD thesis; Université de Paris-Sud, Centre d'Orsay, France 1996.

[7] D. Geman, G. Reynolds. Constrained restoration and the recovery of discontinuities. *IEEE Trans. Pattern Analysis, Machine Intelligence*, vol. 14 : 367-383, 1992.

[8] Y. Zhang, J. A. Fessler, N. H. Clinthorne, W. L. Rogers. Incorporating MRI region information into SPECT reconstruction using joint estimation. *Proc. Int. Conf. ASSP,* Detroit, Michigan, 1995.

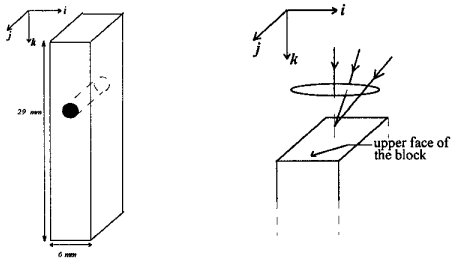

Fig. 3. The inspected block and the source's positions.

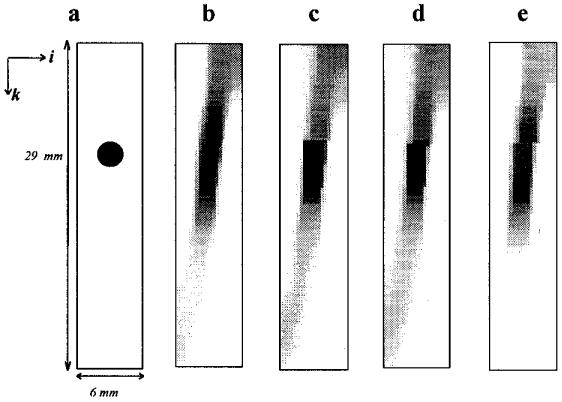

Fig. 4. Vertical cuts of the reconstructed attenuation.
a: ideal cut; **b**: reconstruction from the sole radiographs; **c**: global fusion for a "perfect" positioning; **d**: global fusion for an "imperfect" position matching (the ultrasonic data are down-shifted); **e**: sequential fusion, for an "imperfect" positioning.

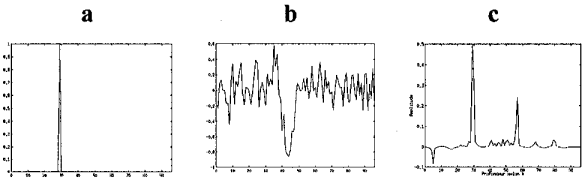

Fig 5. a: Initial reflectivity; b: typical ultrasonic trace; c: recovered reflectivity.